Available online at www.sciencedirect.com

ScienceDirect

journal homepage: http://www.elsevier.com/locate/acme

Original Research Article

On reliable predicting risk and nature of thermal spalling in heated concrete

Dariusz Gawin [a,*], *Francesco Pesavento* [b], *Angel Guerrero Castells* [c]

[a] *Łódź University of Technology, Department of Building Physics and Building Materials, Al. Politechniki 6, 90-924 Łódź, Poland*

[b] *University of Padova, Department of Civil, Environmental and Architectural Engineering, via Marzolo 9, 35131 Padova, Italy*

[c] *Ignia, Cl. Aragón 67, Ibiza, Baleares, Spain*

ARTICLE INFO

Article history:
Received 15 July 2017
Accepted 18 January 2018
Available online 11 April 2018

Keywords:
Thermal spalling
Heated concrete
Numerical simulations
Energetic analysis
Porous media mechanics

ABSTRACT

Thermal spalling is a deterioration phenomenon which is of fundamental importance during durability analysis of concrete structures exposed to high temperature, e.g. during a fire. To assess the risk of this damage mechanism for a real concrete structure, numerical simulations are usually applied since experimental tests are very costly. Some aspects related to predicting thermal spalling by means of numerical modelling of chemo-hygro-thermal and damage processes in heated concrete, are presented in this work. First, we propose a spalling index, validate it with some experimental results and show how it can be used in the quantitative assessment of spalling risk. Then, the results of numerical simulations of a slab, made of two types of concrete (NSC and HPC), heated with three different rates, are discussed from the energetic point of view in order to indicate the main physical causes and predict the nature of thermal spalling: slow, rapid or violent. The presented results allow to assess the contribution of energy due to constrained thermal strains and compressed pore gas into the thermal spalling for different types of concrete heated with different rates.

1. Introduction

Reliable prediction of durability and safety of concrete structures during a fire is of great practical importance, especially when designing concrete elements of high rise buildings or concrete lining of tunnels [1–3]. During heating of such structures, especially with a high rate, their integrity is endangered by the so-called thermal spalling. This paper addresses some issues concerning numerical simulations and prediction of this phenomenon (i.e. the interpretation and application of the numerical results), providing some possible solutions. The phenomenon of spalling is briefly described in Section 2. To assess the risk of thermal spalling occurrence for a concrete structure exposed to heating under given conditions, the evolutions of temperature, moisture content, pore

* *Corresponding author.*
E-mail addresses: dariusz.gawin@p.lodz.pl (D. Gawin), francesco.pesavento@dicea.unipd.it (F. Pesavento), agc@ignia.es (A.G. Castells).
https://doi.org/10.1016/j.acme.2018.01.013
1644-9665/

pressure in the material and the degradation of its mechanical properties, should be known. To predict them with a sufficient accuracy, rather complex mathematical models are required taking into account the multiphysics nature of the system under consideration. Several models of such type were developed in the last twenty years, see e.g. [1,4–14]. One of the state-of-the-art mathematical models of concrete at high temperature was developed by Gawin et al. [9,11,12]. It was widely validated experimentally within some European Projects, e.g. *High Temperature Concrete – HITECO, Upgrading Existing Tunnels – UPTUN*. The model is based on Multiphase Porous Media Mechanics (MPMM). It takes into account several components and phases in the pore network, phase changes, the interactions between physicochemical processes, the transition through the critical point of water [8], as well as the most important material nonlinearities [9]. In Section 3 the main assumptions of this mathematical model are briefly summarized. In Section 4 we describe how the results of numerical simulations can be interpreted in order to assess quantitatively the thermal spalling risk. The analysis is based on the data from real laboratory tests, which are first numerically simulated and then appropriately elaborated. The evolutions of temperature, gas pressure, mechanical damage (concrete cracking) and constrained elastic energy fields are analyzed, in order to propose and validate a parameter (called spalling index) for assessment of the spalling risk occurrence in heated concrete.

Section 5 presents an analysis of the energy accumulated and then released during heating (with three different rates) of a slab made of two types of concrete, what allows to indicate the main physical causes of thermal spalling and to predict its nature (slow or violent or explosive) in the considered cases.

In the last section, some concluding remarks concerning the proposed energetic analysis of the results of numerical simulation are presented for predicting slow/violent/explosive nature of thermal spalling in heated concrete structures.

2. Thermal spalling of concrete

Spalling, in its most general form, is defined as the violent or non-violent breaking off of pieces (or layers) of concrete from the surface of a structural element when it is exposed to rising temperatures, e.g. during a fire [15–18]. A common classification of spalling phenomena leads to identifying the following five main types [16]: Violent Spalling, Sloughing Off, Corner Spalling, Explosive Spalling and Post-Cooling Spalling. Among them, one of the most dangerous is Explosive Spalling, which results in serious loss of material. Explosive Spalling is a very violent form of thermal spalling characterized by the forcible separation of pieces of concrete (the thickness of spalled-off concrete layer is usually of 0.5–2.0 cm [2]), accompanied by a typically loud explosive noise. It normally occurs above the temperature of 200 °C and is stochastic.

For concrete specimens from the same batch and under identical conditions, some could spall while others do not, e.g. [2,11]. Under suitable conditions, in terms of mechanical (external load stress) and thermal load (heating rate), all concretes can show the capacity for thermal spalling.

Spalling is due to different concomitant coupled processes: thermal (heat transfer), chemical (dehydration of cement products and the resulting water release), hygral (water mass transfer, in both liquid and vapor form, and pore pressure build up) and mechanical ones (release of the elastic energy stored during heating and loading and buckling effects in the external layer).

Velocity of spalled-off concrete pieces in fire conditions often exceeds 10 m/s [2], and for explosive spalling even 15 m/s. Considering the possible thickness of spalled-off concrete pieces (0.5–2.0 cm), the kinetic energy of 1 m^2 spalled concrete layer may reach 500–2000 J/m^2, and for explosive spalling even exceed 4500 J/m^2 [11]. Considering possible dimensions and mass of spalled-off concrete pieces (even greater than 0.1 kg), kinetic energy of a single piece may exceed 1 J, what creates the threat to people.

The extent, severity and nature of spalling occurrence are extremely varied. Spalling may be insignificant in amount and consequence, such as when surface pitting occurs. Alternatively, it can have a serious effect on the fire resistance of a structural element because of extensive removal of concrete which exposes the core of the section, and the reinforcing steel or tendons, to a more rapid rise of temperature, thus reducing the load-bearing cross-sectional area, like in the case of explosive spalling. These situations are emphasized and then much riskier in the case of High Performance and Ultra High Performance concrete. Their compactness and special composition result in high values of pore pressure and in a brittle behaviour of the matrix. To reduce the risk of concrete thermal spalling, some preventive measures may be applied [19,20], i.e. concrete of higher permeability (i.e. with higher w/c, without micro-silica) and/or addition of polypropylene fibres to concrete mix (up to 3 kg/m^3) in order to reduce pore pressure; protective layer made of a highly porous material (e.g. shotcrete or special plates) – to reduce heating rate of structure surface; aggregates of low thermal expansion – to reduce concrete cracking during heating. Then special protective steel nets may be applied on a structure surface to protect against spalled concrete pieces having high velocity (kinetic energy) [19].

3. Modelling thermal spalling

The model used in this work was formulated first in the framework of Hybrid Mixture Theories, and then extended to the Thermodynamically Constrained Averaging Theory [21], by considering cementitious materials as multiphase porous media and by supposing that all the phases and components are under equilibrium conditions [8,10,11]. The most important mutual couplings and material nonlinearities, as well as different physical behaviour of water above its critical temperature are taken into account. The model was extensively validated and its constitutive relationships were experimentally determined, e.g. [9,11,17]. The state of the material is described by 4 primary physical quantities, which are also the degrees of freedom in the FE code: gas pressure, p^g, capillary pressure, p^c, temperature, T, and displacement vector, $\mathbf{u}$. In addition, there is a set of internal parameters describing the advancement of the dehydration and deterioration

processes, i.e. degree of dehydration, Γ_{dehydr}, chemical damage parameter, V, and mechanical damage parameter, d [9,22].

The main steps needed for the development of such mathematical model are beyond the scope of this work, so here we limit to presenting the main governing equations.

- *Mass balance equation of dry air*:

$$-n\frac{\partial S_w}{\partial t}-\beta_s(1-n)S_g\frac{\partial T}{\partial t}+S_g\nabla\cdot v^s+\frac{S_g n}{\rho^{ga}}\frac{\partial \rho^{ga}}{\partial t}+\frac{1}{\rho^{ga}}\nabla\cdot J_g^{ga}+\frac{1}{\rho^{ga}}\nabla\cdot\left(n S_g\rho^{ga}v^{gs}\right)-\frac{(1-n)S_g}{\rho^s}\frac{\partial \rho^s}{\partial \Gamma_{dehydr}}\frac{\partial \Gamma_{dehydr}}{\partial t}=\frac{\dot{m}_{dehydr}}{\rho^s}S_g \quad (1)$$

where n is the porosity, t – time, S_π – saturation, β_π – thermal expansion coefficient, ρ^π – density, $\dot{m}_{dehydr}$ – mass source term related to the dehydration process, Γ_{dehydr} – dehydration process degree, $\mathbf{v}^{\pi s}$ – velocity relative to the solid skeleton, J_g^{ga} – diffusive flux of dry air in water vapor. The subscripts/superscripts ($\pi = s$, ga, gw and g) are related to solid, dry air, water vapor and gas phase, respectively.

- *Mass balance equation of water species (water vapour + liquid water)*:

$$n(\rho^w-\rho^{gw})\frac{\partial S_w}{\partial t}+(\rho^w S_w+\rho^{gw}S_g)\alpha\nabla\cdot\mathbf{v}^s-\beta_{swg}\frac{\partial T}{\partial t}+S_g n\frac{\partial \rho^{gw}}{\partial t}+\nabla\cdot\mathbf{J}_g^{gw}+\nabla\cdot\left(n S_w\rho^w\mathbf{v}^{ws}\right)+\nabla\cdot\left(n S_g\rho^{gw}\mathbf{v}^{gs}\right)-\left(\rho^w S_w+\rho^{gw}S_g\right)\frac{(1-n)}{\rho^s}\frac{\partial \rho^s}{\partial \Gamma_{dehydr}}\frac{\partial \Gamma_{dehydr}}{\partial t}=\frac{\dot{m}_{dehydr}}{\rho^s}\left(\rho^w S_w+\rho^{gw}S_g-\rho^s\right) \quad (2)$$

where α is the Biot constant, J_g^{gw} – diffusive flux of water vapor in dry air.

- Energy balance equation of the multiphase system:

$$(\rho C_p)_{eff}\frac{\partial T}{\partial t}+\left(\rho_w C_p^w\mathbf{v}^w+\rho_g C_p^g\mathbf{v}^g\right)\cdot\nabla T-\nabla\cdot(\lambda_{eff}\nabla T)=-\dot{m}_{vap}\Delta H_{vap}+\dot{m}_{dehydr}\Delta H_{dehydr} \quad (3)$$

where $(\rho C_p)_{eff}$ is effective thermal capacity of the multiphase system, C_p – isobaric specific heat, λ_{eff} – effective thermal conductivity, ΔH_{vap} and ΔH_{dehydr} – specific enthalpies of the phase change (evaporation–condensation) and dehydration, $\dot{m}_{vap}$ – the mass source term related to water vaporisation.

- *Linear momentum balance equation*:

$$\nabla\cdot[(1-d)(1-V)\mathbf{\Lambda}_0:(\boldsymbol{\varepsilon}_{tot}-\boldsymbol{\varepsilon}_{th}-\boldsymbol{\varepsilon}_{tchem}-\boldsymbol{\varepsilon}_{tr})-\alpha p^s\mathbf{I}]+\rho\mathbf{g}=0 \quad (4)$$

where ρ is the porous medium density, p^s is a measure of the so-called solid pressure, i.e. the pressure exerted by the fluid phases on the solid skeleton, $\boldsymbol{\varepsilon}_{tot}$ is the total strain, $\boldsymbol{\varepsilon}_{th}$ – thermal strain, $\boldsymbol{\varepsilon}_{tchem}$ – chemical strain and $\boldsymbol{\varepsilon}_{tr}$ – transient thermal strain, $\mathbf{\Lambda_0}$ is the elastic stiffness tensor, $d = f[\boldsymbol{\sigma}_e^s(\mathbf{x},t)]$ and $V = f[T_{max}(\mathbf{x}, t)]$ are the mechanical and thermo-chemical damage parameters, respectively. $\boldsymbol{\sigma}_e^s$ is the effective stress tensor which is responsible for the deformation of the material, is the maximal temperature reached at a given point $\mathbf{x}$ till time instant t.

The full mathematical model and details of its numerical solution can be found in previous works [9,11,12,17].

4. Predicting thermal spalling by means of numerical simulations

In order to evaluate quantitatively the risk of thermal spalling occurrence in concrete structures, heated at given conditions, some special indexes have been proposed in [11]. They have been proven to give a reliable assessment of the risk for the MIX1 and MIX2 concrete specimens heated up to 450 °C during the unloaded tests at NIST [11]. The cylindrical specimens (with diameter of 100 mm and height of 200 mm) were heated with the rate of 5 K/min to three target temperatures: 300 °C, 450 °C and 600 °C.

For the MIX1 specimen (with $w/c = 0.22$, compressive strength $f_c = 98$ MPa and intrinsic permeability $k_0 = 2\times10^{-19}$ m^2) heated to 300 °C (indicated later on as MIX1/300 °C) thermal spalling occurred for none of the three specimens, but during heating to 450 °C it was observed for each of the three specimens. Whereas every of the three MIX 2 specimens ($w/c = 0.33$, $f_c = 88$ MPa, $k_0 = 22\times10^{-18}$ m^2) experienced explosive spalling during heating to 600 °C, while during the 450 °C tests it occurred only for one of the four specimens. Main material properties of the MIX1 and MIX 2, the FE mesh, as well as initial and boundary conditions used in our simulations are given in detail in [11].

Here two of the previously proposed indexes [11], accounting for commonly accepted factors promoting concrete spalling, i.e. high gas pressure, material cracking (mechanical damage) and high constrained elastic energy, are jointly used for defining a unique spalling index. It seems to give an assessment of spalling risk in heated concrete better than the previous ones [11], as will be shown below.

The first spalling index, I_{s1}, is based on the pressure-induced shear mechanism:

$$I_{s1}=A_{g1}\frac{(p^g-p_{atm})d}{\bar{f}_t}, \quad (5)$$

where $\bar{f}_t$ is the averaged traction strength, p_{atm} the atmospheric pressure, p^g and d, are the local values of gas pressure and mechanical damage parameter. The over-bar means the value averaged along the distance between the current position and the heated surface and the term A_{g1} is a geometry dependent coefficient [11]. The index I_{s1} assumes high gas pressure accompanied by concrete cracking and degradation of its traction strength as main causes of thermal spalling.

The second spalling indexes, I_{s2}, is based on fracture mechanics:

$$I_{s2}=A_{g2}\frac{\bar{E}_{el}d}{\bar{G}_f}, \quad (6)$$

where the constrained elastic energy $\overline{E}_{el}$ and the fracture energy $\overline{G}_f$, are averaged over the distance from the heated surface to a given position (i.e. a possible thickness of spalled concrete layer), while the term A_{g2} is a geometry dependent coefficient [11]. This spalling index considers the constrained elastic energy of the material layer close to heated surface, accompanied by cracking of the layer and decrease of its fracture energy, as prevailing causes of the phenomenon.

Since it is usually impossible to predict in advance which physical phenomenon will be dominant in development of thermal spalling at given conditions, it seems reasonable to assume that the higher value of the two spalling indexes at a given position and time instant, should be taken to assess risk of the phenomenon occurrence,

$$I_{\sup}(\mathbf{x},t) = \sup(I_{s1}(\mathbf{x},t); I_{s2}(\mathbf{x},t)), \tag{7}$$

where I_{sup} will be called the supremum spalling index, t means the time instant and $\mathbf{x}$ the position vector.

To validate this concept, again the results of numerical simulations of the NIST laboratory tests [23] for the all four aforementioned cases (i.e. MIX1/300 °C, MIX1/450 °C, MIX2/450 °C and MIX2/600 °C), will be used. The results for the MIX1/450 °C case, were used in [11] to determine the geometry parameters in Eqs. (1) and (2) in such a way that the maximal values of the spalling indexes I_{s1} and I_{s2} for the whole simulated test were equal to one. It is worth to mention that these indexes reached their maximal values in the time period when thermal spalling really occurred during the NIST tests [23]. Here, using the results of simulations performed, the indexes, I_{s1}, I_{s2} and I_{sup}, for the all analyzed concrete mixtures and temperatures, are calculated. For brevity, only the results concerning the evolutions of spalling index I_{sup} during the tests performed for the MIX-1, Fig. 1(a and b), and MIX-2, Fig. 1(c and d), heated up to the analyzed target temperatures, are presented. Additionally, the results concerning evolution of mechanical damage in 4 points of the specimen made of the MIX-1 are shown in Fig. 2(a and b) and of the MIX-2 in Fig. 2(c and d), since they are useful for proper assessment of thermal spalling risk.

For the MIX-1/300 °C case, after about 120 min of heating the highest level of spalling index $I_{sup} \approx 0.63$ was reached in the central part of specimen, while in its surface layer the index

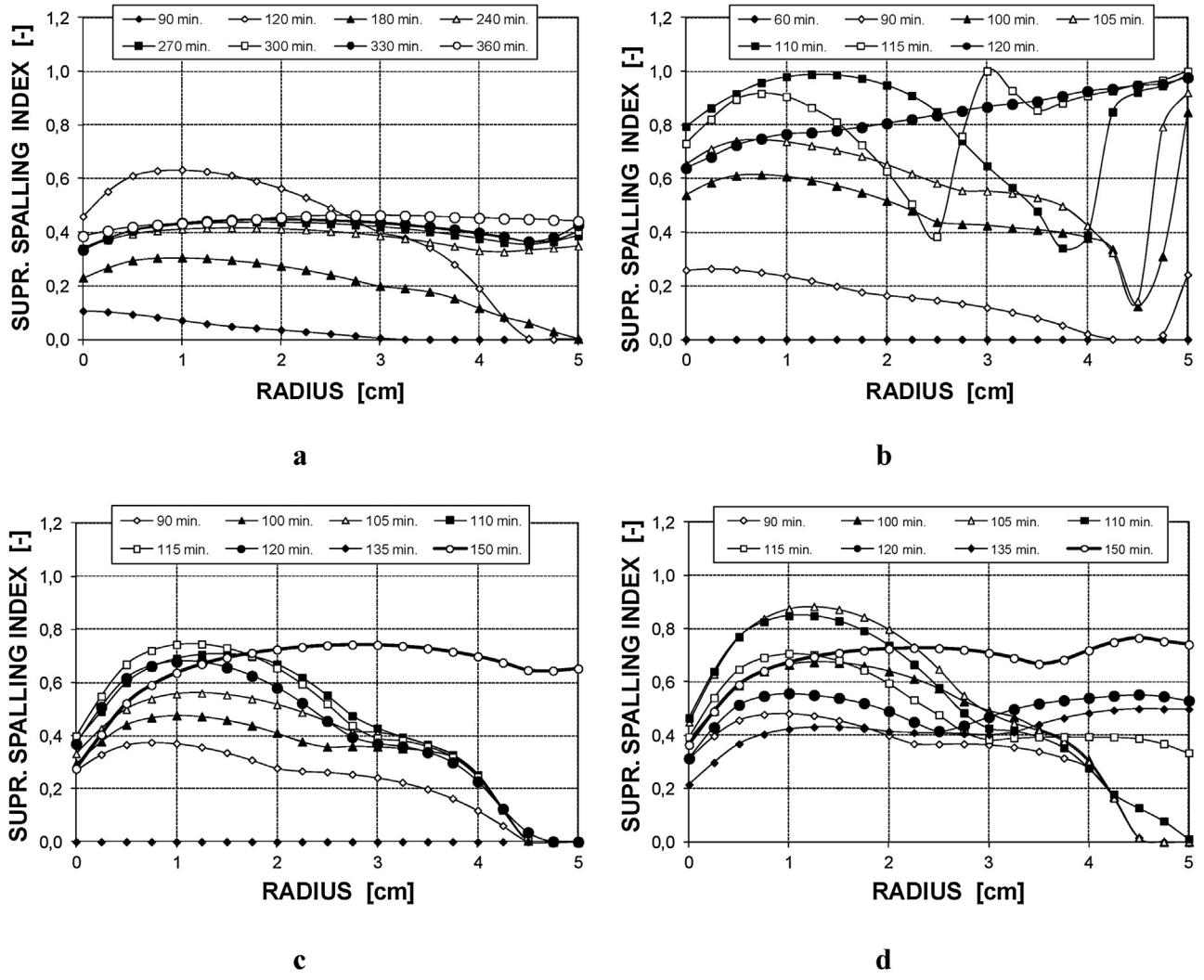

Fig. 1 – The evolutions of spalling index I_{sup} during the NIST unloaded heating tests [23]: (a) MIX-1/300 °C; (b) MIX-1/450 °C; (c) MIX-2/450 °C; (d) MIX-2/600 °C.

remained at low level, Fig. 1a. In the same time period the mechanical damage parameter was not increasing, Fig. 2a. During the laboratory tests, thermal spalling was registered for none of the three MIX-1 specimens.

For the MIX-1/450 °C case, after 110–115 min of heating the spalling index I_{sup} reached values close to 1.0 in the central part of specimen and in its 2-cm surface layer, Fig. 1b. In this time period the mechanical damage was increasing with the rate of about 30% per minute, starting from the inner part of specimen, see Fig. 2b. During the laboratory tests for all of the three specimens explosive spalling occurred.

For the MIX-2/450 °C case, after about 115 min of heating the spalling index reached its highest level $I_{sup} \approx 0.75$ in the specimen central part, while near the surface its level was relatively low, Fig. 1c. In the same time period the mechanical damage remained at a low and constant level, Fig. 2c, but from 120 min it started increasing gradually (with the rate of about 1% per minute), together in the whole surface zone of the specimen. This was accompanied by a gradual increase of the spalling index value to about 0.7 in the whole specimen. During the laboratory tests, explosive spalling was observed for one of the four MIX-2 specimens.

For the MIX-2/600 °C case, after 110–115 min of heating the spalling index I_{sup} in the specimen central part reached value of about 0.9 and during next 10 min its value in the surface layer increased to about 0.55, Fig. 1d. In the same time period the damage parameter was increasing with the rate of about 2% per minute, together in the whole surface layer, Fig. 2d. During the laboratory tests, explosive spalling was observed for all of the three MIX-2 specimens.

One can notice a good agreement of the spalling risk assessment based on the index I_{sup} and evolution of mechanical damage obtained from the numerical simulation, with the real NIST experimental observations [23]. Thermal spalling occurred in the tested concrete specimens, when the index I_{sup} reached the level of 0.9–1.0 and at the same time mechanical damage parameter, being initially at relatively low level ($d \approx 25\%$) in the surface layer, was increasing with a high

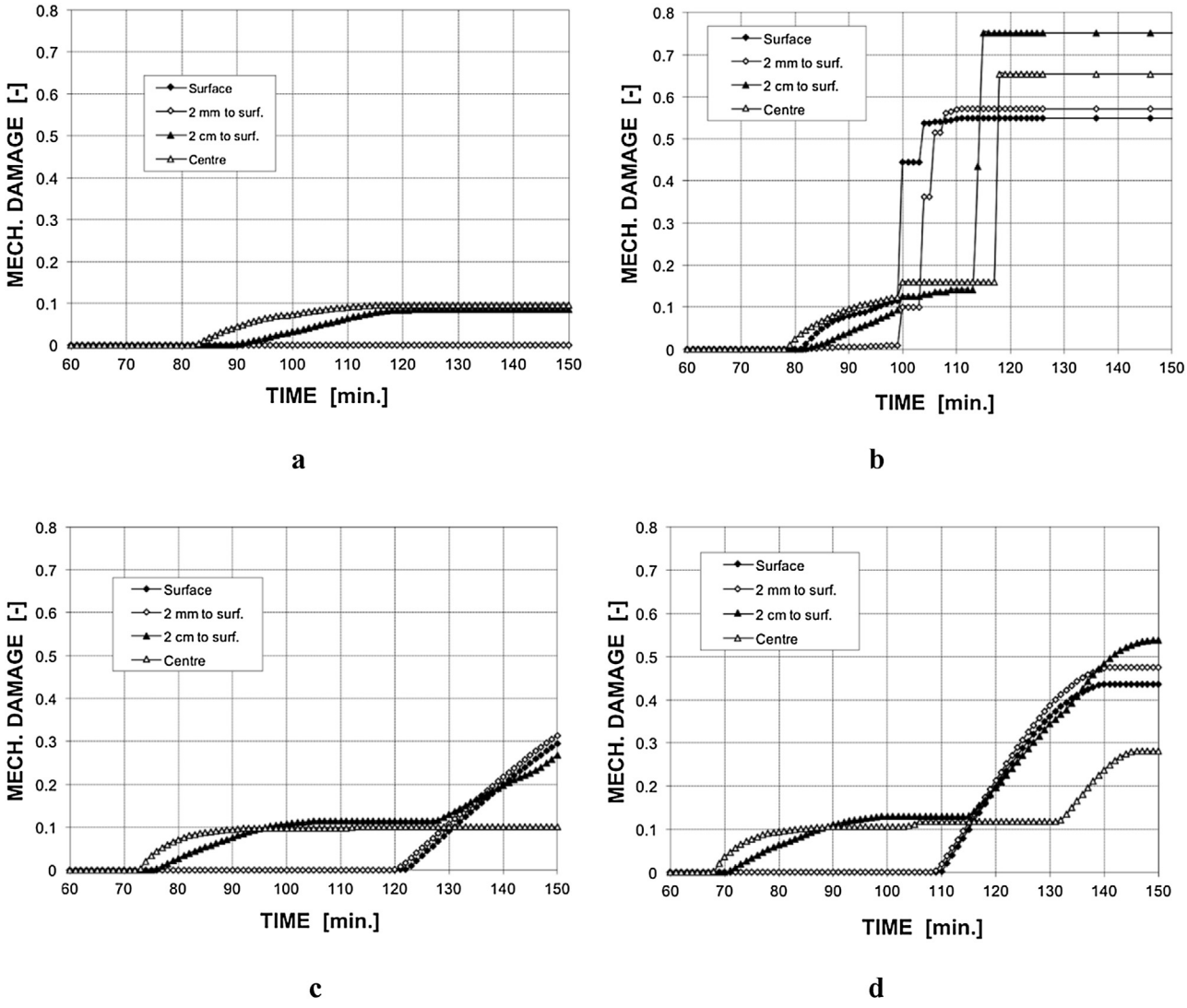

Fig. 2 – The time evolutions of mechanical damage in 4 points of the cylindrical concrete specimens during the NIST tests [23]: (a) MIX-1/300 °C; (b) MIX-1/450 °C; (c) MIX-2/450 °C; (d) MIX-2/600 °C.

rate, together in the whole layer. The I_{sup} index exceeding 0.75, accompanied by a relatively low ($d \approx 15$–25%), slowly increasing mechanical damage level in the surface layer, corresponded to relatively low risk of thermal spalling (it occurred for one of the four specimens). The spalling events were observed in the temperature range between ≈200 °C and ≈250 °C. For the lower values of index I_{sup} and not increasing mechanical damage parameter, both in the inner and surface layers of the specimens, thermal spalling was not observed.

The above observations indicate that the simulation results performed by means of the numerical model of heated concrete [9] and the spalling analysis based on the evolutions of the I_{sup} index and mechanical damage parameter, may be useful when evaluating thermal spalling risk. To assess, if thermal spalling will be of explosive or progressing nature, an energetic analysis should be performed, similarly to what is presented in Section 5.

5. Energetic analysis of thermal spalling in concrete heated with different rates

In this section, we numerically analyze the energetic viability of concrete spalling and its expected nature (either violent/explosive or slow). The scope is also to discern what is the energy contribution of compressed gas (caused by rapid evaporation of moisture) and what is that corresponding to the release of stored constrained elastic energy (due to the thermal stresses resulting from high restrained strains caused by temperature gradients). The study is performed for a slab, made of two different types of concrete and exposed to three different parametric heating profiles (with distinctly different heating rates, variable in time).

Once the time and the position of the potential main fracture are determined by analysis of the simulations results, it is possible to determine if concrete spalling is energetically possible through the comparison between fracture energy and the stored elastic energy, similarly as in [11]. At this stage, it is also possible to assess the contribution to spalling occurrence of both the work of initially compressed gas during its rapid expansion and of the constrained elastic energy, as well as to evaluate the expected nature of spalling (either violent/explosive or slow). The latter can be achieved through the calculation of the velocity of the spalled concrete pieces, following the procedure proposed in [11].

The analysis of spalling occurrence is performed for a concrete wall, which is assumed to work in plain strain conditions with 1-D flow of both heat and mass.

The boundary conditions used in numerical simulation are summarized in Table 1 (the structural element is exposed to fire at one face only). For the heat exchange on the side A of the slab (exposed to fire), both convective and radiative conditions are considered, while on the opposite side B purely convective exchange is assumed. The heat exchange coefficients are derived from [11].

The heating profiles considered for the side A of the slab are derived directly from the Annex A of the Eurocode 1 [24], in which some parametric curves are defined on experimental basis, considering: the fire load density, the ventilation conditions (i.e. geometry, size and distribution of the compartment openings), the properties of the closing walls of the fire compartment (walls thermal capacity and limit of the fire temperature).

The heating profiles $T_g(t)$, defining the air temperature T_g [K] within the fire sector, are given by the following equation [24]:

$$T_g(t) = 293.15 + 1325\cdot(1-0.324\cdot e^{-0.2\cdot\Gamma\cdot t}-0.204\cdot e^{-1.7\cdot\Gamma\cdot t}-0.472\cdot e^{-19\cdot\Gamma\cdot t}), \quad (8)$$

where t [h] – time, $\Gamma = (O/b)^2/(0.04/1160)^2$ [J/(m^{2}s$^{1/2}$K)], $b = \sqrt{\rho\cdot c\cdot\lambda}$ is the parameter dependent on the density – ρ, the specific heat – c, and the thermal conductivity – λ of the element closing the fire sector, which is assumed here as b = 2016 J/(m^{2}s$^{1/2}$K), $O = A_v\cdot\sqrt{h_{eq}}/A_t$ [m$^{1/2}$] is the opening coefficient, dependent on the total surface and the average height of the vertical openings at all of the walls, A_v [m^2] and h_{eq} [m], and the total surface closing the fire sector, including openings, A_t [m^2].

Table 1 – Boundary conditions used in the numerical simulation.

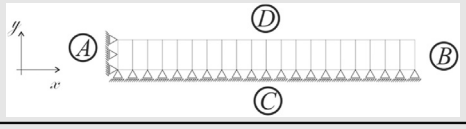

Side	Variables	Coefficients
A	p^g	p^g = 101,325 Pa
	p^c	p^{gw} = 1300 Pa, convective mass exchange coefficient β_c = 0.02 m/s
	T	$T = T(t)$ – according to three different heating profiles
		Convective heat exchange coefficient: α_c = 20 W/m^2 K;
		Radiative heat exchange coefficient: $e\sigma_0 = 5.1\times10^{-8}$ W m^{-2} K^{-1}
B	u_x	$u_x = 0$
	p^g	p^g = 101,325 Pa
	p^c	Environmental relative humidity = 50%, β_c = 0.005 m/s
	T	Convective BC: ambient temperature T = 298.15 K, α_c = 5 W/m^2 K
C, D	u_y	$u_y = 0$, $q_y{}^T = 0$, $q_y{}^g = 0$, $q_y{}^w = 0$,

The considered heating profiles have been obtained by varying the opening coefficient, O, as follows:

(a) Slow Parametric Fire, Eq. (8) with O = 0.02 $m^{1/2}$ (geometry, size and distribution of the assumed compartment openings are given in [25]), represents a slow development fire that reaches its maximum temperature after about 3 h;
(b) ISO-Fire 834, Eq. (8) with O = 0.07 $m^{1/2}$, is the normalized ISO 834 time–temperature curve defined in the regulation project prEN 13501-2 to represent a fire model completely developed in a fire sector;
(c) Hydrocarbon Fire, is the normalized time-temperature curve defined in [24], which represents the fire conditions where hydrocarbon products are present; it is given by the following equation:

$$T_g(t) = 293.15 + 1080\cdot(1-0.325\cdot e^{-0.167\cdot t\cdot 60}-0.675\cdot e^{-2.5\cdot t\cdot 60}). \quad (9)$$

A comparison between the three considered heating profiles is shown in Fig. 3 and the main physical properties (at ambient temperature of 20 °C) of the two concretes, NSC and HPC, considered in the analysis, are listed in Table 2.

The simulation results, concerning main physical quantities at the time instant and position of predicted spalling occurrence are presented in Table 3 and the results of energetic analysis performed following procedure [11] are compared in Table 4. For brevity, the detailed results of time evolutions and space distributions of the physical quantities and spalling indexes, used in the analyses, are not presented here and can be found in [25]. The spalling occurrence (i.e. its position and time) was assumed to take place following the procedure described in Section 4, i.e. based on the value of index I_{sup} and the rate of mechanical damage increase, obtained from the numerical simulation [25].

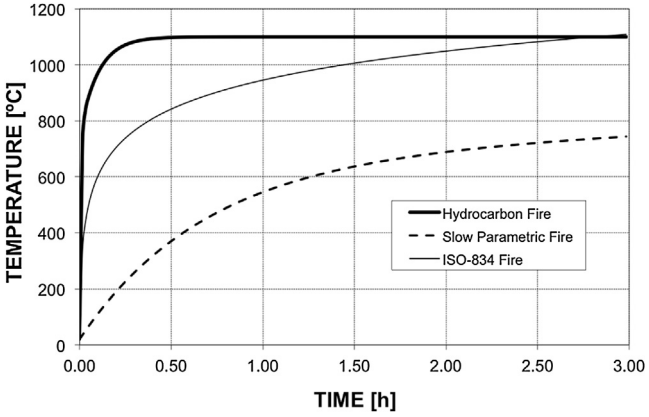

Fig. 3 – Graphical comparison of the considered heating profiles according to [24]: ISO-834 Fire (Eq. (8) with the parameters in point b), Slow Parametric Fire (Eq. (8) with the parameters in point a) and Hydrocarbon Fire (Eq. (9)).

Table 2 – Main properties of the considered concretes at ambient temperature.

Material property	NSC	HPC
MIP porosity, n [%]	9.0	6.0
Water intrinsic permeability, k_o [m^2]	1×10^{-17}	1×10^{-19}
Young modulus, E [GPa]	34.5	36.7
Poisson's ratio, ν [–]	0.18	0.18
Thermal conductivity, λ [W/m K]	1.95	2.1
Specific heat, C_p [J/kg K]	851	851

As can be observed in Tables 3 and 4, the characteristics of thermal spalling are strongly dependent both on the concrete properties and the heating rate. Nevertheless, some general trends, being in a good agreement with the published data on laboratory tests and field observations [2,23,26] (including the measured values of velocity of spalled pieces of heated concrete slab [26]), can be deduced from these results.

In concretes characterized by a higher value of permeability (porosity), e.g. NSC concrete, the constrained elastic energy due to temperature gradient in a layer close to heated surface plays a dominant role in the development of thermal spalling (the value of spalling index I_{s2} is crucial). Gas pressure, even at high heating rates, is less important. On the contrary, in a tighter concrete, e.g. HPC concrete, a high gas pressure due to rapid moisture evaporation during heating (i.e. spalling index I_{s1}) is a dominant factor causing concrete spalling. The higher heating rate is, the more important for the phenomenon occurrence is high gas pressure. Only during slow heating of these concretes, the roles played by high pressure and constrained elastic energy are comparable. For both types of concrete, the higher heating rate is applied, the higher velocity (i.e. more violent process) and smaller thickness of spalled pieces of concrete can be expected. In the case of very high heating rates (e.g. during hydrocarbon fire) in very tight concrete (e.g. HPC or UHPC) one can expect explosive spalling occurrence. The higher heating rate is, the higher is temperature of the spalled concrete layer.

The proposed here method of thermal spalling analysis allows for better understanding of the phenomenon development in different heating conditions and predicting its some most practically important characteristics, like time and temperature range of possible occurrence, kinetic energy of concrete pieces, thickness of spalled concrete layer. The results of such analysis can be useful during assessment of a concrete structure durability for different scenarios of fire or accident situation.

6. Conclusions

Some issues related to application of numerical models, and the interpretation of their results, for assessment of thermal spalling risk in heated concrete structures have been discussed. The analyses presented previously [9,11,12] and in this work have shown that numerical simulations can be a useful tool for assessment of thermal spalling risk, under condition that they are performed with an experimentally validated computer code, based on a sufficiently accurate mathematical model of hygro-thermal, thermo-chemical, stress–strain and degradation processes in heated concrete.

The evolutions of temperature, gas pressure, mechanical damage (concrete cracking) and constrained elastic energy

Table 3 – Results of spalling analysis for the considered types of concrete and heating profiles.

Concrete	Heating profile	Spalling time [min]	Abs. max	Value at (first) spalling fracture position				
			p^g [bar]	x [cm]	p^g [bar]	T [K]	d [–]	I_{sup} [–]
NSC	Slow Parametric Fire	40–50	4.05	~2.0	3.12	476	0.51	0.36
	ISO-Fire 834	10–12	6.52	~1.2	5.28	485	0.41	0.63
	Hydrocarbon Fire	5–7	11.9	~0.7	2.44	819	0.31	0.97
HPC	Slow Parametric Fire	50–68	13.4	~1.3	8.80	513	0.70	0.45
	ISO-Fire 834	8–10	26.2	~1.0	14.5	516	0.60	0.79
	Hydrocarbon Fire	3–6	48.3	~0.5	21.3	710	0.46	0.99

Table 4 – Results of energy analysis for the considered types of concrete and heating profiles.

Concrete	Heating profile	ΔU [J/m^2]	W [J/m^2]	ΔE_k [J/m^2]	v [m/s]	Gas work contribution [%]	Elast. energy contribution [%]
NSC	Slow parametric fire	742	86	223	3.8[a]	10.4%	89.6%
	ISO-Fire 834	674	192	264	5.8[b]	22.2%	77.8%
	Hydrocarbon fire	717	68	184	8.4[b]	8.7%	91.3%
HPC	Slow parametric fire	301	421	119	3.6[a]	58.3%	41.7%
	ISO-Fire 834	327	731	457	9.3[b]	69.1%	30.9%
	Hydrocarbon fire	149	1569	1118	29.2[c]	91.3%	8.7%

[a] Slow spalling.
[b] Violent spalling.
[c] Explosive spalling.

fields provide sufficient information for a quantitative spalling risk assessment, for example by means of the approach and spalling index proposed here.

The simulations confirmed some general trends concerning causes of thermal spalling and its slow or violent nature, being in a good agreement with some known laboratory tests and field observations. In concrete characterized by a higher value of permeability, e.g. NSC concrete, the constrained elastic energy due to temperature gradient in a layer close to heated surface plays a dominant role in the development of thermal spalling, while gas pressure, even at high heating rates, is less important. On the contrary, in a tighter concrete, e.g. HPC concrete, a high gas pressure due to rapid moisture evaporation during heating is a dominant cause of concrete spalling. The higher heating rate is, the more important for the phenomenon occurrence is high gas pressure. Only during slow heating of relatively tight concretes, the roles played by high pore pressure and constrained elastic energy are comparable. For the both types of concrete, the higher heating rate is applied, the more violent character of the phenomenon.

The performed study, based on the data of the real laboratory tests as well as on the proposed here spalling index and analysis of the energy released during thermal spalling [1], confirmed that the results of numerical simulations of heated concrete structures can be appropriately interpreted to evaluate thermal spalling risk, and predict nature (slow, violent or explosive) of the phenomenon.

Ethical statement

Authors state that the research was conducted according to ethical standards.

Acknowledgements

None.

Funding body: The research was partly supported by the project POIG.01.01.02-10-106/09-00 at the Lodz University of Technology, Poland, within the ''Innovative Economy Strategic Programme'' funded by the European Union, and partly by the project CPDA 135049 funded by the University of Padova, Italy.

REFERENCES

[1] Z.P. Bazant, M.F. Kaplan, Concrete at High Temperatures: Material Properties and Mathematical Models, Longman, Harlow, 1996.
[2] L.T. Phan, N.J. Carino, D. Duthinh, E. Garboczi (Eds.), Proceedings of International Workshop on Fire Performance of High-Strength Concrete, NIST Special Publication 919Gaitherburg (USA), 1997.
[3] T. Ring, M. Zeiml, R. Lackner, Underground concrete frame structures subjected to fire loading: Part I – Large-scale fire tests, Eng. Struct. 58 (2014) 175–187.
[4] C.T. Davie, C.J. Pearce, N. Bicanic, Coupled heat and moisture transport in concrete at elevated temperatures – effects of capillary pressure and adsorbed water, Numer. Heat Transf. 49 (2006) 733–763.
[5] C.T. Davie, C.J. Pearce, N. Bićanić, A fully generalised, coupled, multi-phase, hygro-thermo-mechanical model for concrete, Mater. Struct. 43 (Suppl. 1) (2010) 13–33.
[6] M.B. Dwaikat, V.K.R. Kodur, Hydrothermal model for predicting fire-induced spalling in concrete structural systems, Fire Saf. J. 44 (2009) 425–434.
[7] G.L. England, N. Khoylou, Moisture flow in concrete under steady state non-uniform temperature states: experimental

observations and theoretical modelling, Nucl. Eng. Des. 156 (1995) 83–107.
[8] D. Gawin, F. Pesavento, B.A. Schrefler, Modelling of hygro-thermal behaviour and damage of concrete at temperature above critical point of water, Int. J. Numer. Anal. Methods Geomech. 26 (6) (2002) 537–562.
[9] D. Gawin, F. Pesavento, B.A. Schrefler, Modelling of thermo-chemical and mechanical damage of concrete at high temperature, Comput. Methods Appl. Mech. Eng. 192 (2003) 1731–1771.
[10] Y. Ichikawa, G.L. England, Prediction of moisture migration and pore pressure build-up in concrete at high temperatures, Nucl. Eng. Des. 228 (2004) 245–259.
[11] D. Gawin, F. Pesavento, B.A. Schrefler, Towards prediction of the thermal spalling risk through a multi-phase porous media model of concrete, Comput. Methods Appl. Mech. Eng. 195 (2006) 5707–5729.
[12] D. Gawin, F. Pesavento, An overview of modeling cement based materials at elevated temperatures with mechanics of multi-phase porous media, Fire Technol. 48 (2012) 753–793.
[13] F. Meftah, S. Dal Pont, Staggered finite volume modeling of transport phenomena in porous materials with convective boundary conditions, Transp. Porous Media 82 (2) (2010) 275–298.
[14] Y. Zhang, M. Zeiml, C. Pichler, R. Lackner, Model-based risk assessment of concrete spalling in tunnel linings under fire loading, Eng. Struct. 77 (2014) 207–215.
[15] G.A. Khoury, Y. Anderberg, Concrete Spalling Review, Fire Safety Design Report, Swedish National Road Administration, 2000.
[16] A.J. Breunese, J.H.H. Fellinger, Spalling of Concrete and Fire Protection of Concrete Structures, TNO Report, Netherlands Organisation for Applied Scientific Research, 2004.
[17] D. Gawin, F. Pesavento, B.A. Schrefler, Modelling of deformations of high strength concrete at elevated temperatures, Mater. Struct. 37 (268) (2004) 218–236.
[18] T. Gernay, A. Millard, J.-M. Franssen, A multiaxial constitutive model for concrete in the fire situation: theoretical formulation, Int. J. Solids Struct. 50 (22–23) (2013) 3659–3673.
[19] EN 1992-1-2:2004, Eurocode 2: Design of concrete structures - Part 1-2: General rules – Structural fire design.
[20] A. Witek, D. Gawin, F. Pesavento, B.A. Schrefler, Finite element analysis of various methods for protection of concrete structures against spalling during fire, Comput. Mech. 39 (2007) 271–292.
[21] W.G. Gray, C.T. Miller, Thermodynamically constrained averaging theory approach for modeling flow and transport phenomena in porous medium systems: 1. Motivation and overview, Adv. Water Resour. 28 (2005) 161–180.
[22] C. de Sa, F. Benboudjema, Modeling of concrete nonlinear mechanical behavior at high temperatures with different damage-based approaches, Mater. Struct. 44 (8) (2011) 1411–1429.
[23] L.T. Phan, R.D. Peacock, Experimental Plan for Testing the Mechanical Properties of High-Strength Concrete at Elevated Temperature, Res. Report NISTIR 6210, National Institute of Standards and Technology, Building and Fire Research Laboratory, Gaithersburg, MD 20899, USA, 1999.
[24] EN 1991-1-2:2002., Eurocode 1, Part 1-2. Actions on Structures. General Actions. Actions on Structures Exposed to Fire, European Standard Organization, 2002.
[25] A.G. Castells, Contribution to the Advanced Analysis and Prevention of the Mechanisms of Natural Fire Induced Structural Collapse in High-rise Buildings, Ph.D. Thesis, Technical University of Catalonia, Barcelona (Spain), 2009.
[26] M. Zeiml, R. Lackner, H. Mang, Experimental insight into spalling behavior of concrete tunnel linings under fire loading, Acta Geotech. 3 (2008) 295–308.